Available online at www.sciencedirect.com
SCIENCE DIRECT®

Journal of the European Ceramic Society 23 (2003) 2307–2314
www.elsevier.com/locate/jeurceramsoc

Influence of deposition parameters on the dielectric properties of rf magnetron sputtered $Ba(Zr_xTi_{1-x})O_3$ thin films

Moo-Chin Wang[a,*], Chung-Yi Chen[b], Chi-Shiung Hsi[c], Nan-Chung Wu[b]

[a]*Department of Mechanical Engineering, National Kaohsiung University of Applied Sciences, 415 Chien-Kung Road, Kaohsiung, 80782, Taiwan*
[b]*Department of Materials Science and Engineering, National Cheng Kung University, 1 Ta-Hsueh Road, Tainan, 70101, Taiwan*
[c]*Department of Materials Science and Engineering, I-Shou University, 1 Hsueh-Cheng Road, Section 1, Ta-Hsu, Kaohsiung, Taiwan*

Received 13 July 2002; received in revised form 6 January 2003; accepted 13 January 2003

Abstract

$Ba(Zr_xTi_{1-x})O_3$ (BZ_xT_{1-x} in short) thin films have been deposited on $Pt/Ti/SiO_2/Si$ substrates by radio frequency magnetron sputtering and their dielectric properties have been characterized as a function of sputtering parameters. The BZ_xT_{1-x} thin films are amorphous when sputtered at rf power (R_p) = 100 W and substrate temperature (S_T) = 300 °C. The crystalline phase of the BZ_xT_{1-x} thin films appears when the substrate temperature increases from 300 to 400 and 500 °C, respectively, and the films have a high degree of (100) preferred orientation. The dielectric constant decreases with increasing measurement temperature, irrespective of the rf power and Zr content of the BZ_xT_{1-x} thin films. The $BZ_{0.3}T_{0.7}$ thin films have a low dielectric loss tangent irrespective of the sputtering parameters. The dielectric constant of the $BZ_{0.3}T_{0.7}$ thin film increases with increasing $Zr\cdot(Zr+Ti)^{-1}$ ratio and deposition temperature but decreases with increasing working pressure. Besides, the dielectric constant suddenly increases from 244.0 to 284.1 when the rf power increases from 100 to 130 W, then it decreases from 284.1 to 270.0 when the rf power increases from 130 to 160 W. The dielectric constant also suddenly increases from 164.1 to 281.5 when the sputtering gas contains O_2 from 0 to 10%, but its variation is insignificant when the sputtering gas contains O_2 from 10 to 20%.

Keywords: $Ba(Zr,Ti)O_3$; Dielectric properties; Sputtering; Thin films

1. Introduction

In recent years, thin films such as $BaTiO_3$,[1,2] $SrTiO_3$,[3–6] $(Ba,Sr)TiO_3$,[7–9] $Pb(Zr,Ti)O_3$,[10] and $(Ba,Pb)(Zr,Ti)O_3$[11,12] with a high relative dielectric constant have been considered for use as storage capacitors in dynamic random access memories (DRAMs), such a dielectric material should have a low leakage current and a high dielectric constant, and it is desirable that it has a paraelectric phase to avoid fatigue due to ferroelectric domain switching.[7] Among the perovskite compounds in the $BaTiO_3$ (BT in short)-$SrTiO_3$ (ST in short) system, $Ba(Sr,Ti)O_3$ (BST in short), is the most promising candidate for the fabrication of memory cell capacitors in DRAMs with very large scale integration and has been extensively studied with respect to the dielectric properties of the paraelectric phase.[9] From a material viewpoint, BST can be categorised as a solution between BT and ST and expressed as xBT-$(1-x)$ST. BT is a ferroelectric material with the Curie temperature of 120 °C, while ST is a paraelectric material with phase transition at approximately −245 °C (Bulk). In the past several years, many studies have been carried out focusing on the deposition techniques and electrical properties of the BST films.[7–9,13–15]

The ferroelectric $Pb(Ti,Zr)O_3$ films with a $Ti\cdot(Zr)^{-1}$ ratio of $50\cdot50^{-1}$ of a thickness ranging from 170 to 210 nm deposited on Pt-coated Si substrates by the multi-ion-beam reactive sputtering system at room temperature and a deposition rate of about 1.8 nm min^{-1}, have been investigated by Krupanidhi et al.[16] Hu and Krupanidhi[10] have reported the use of low-energy oxygen ion bombardment to enhance the electrical properties of multi-ion beam sputter deposited ferroelectric $Pb(Ti,Zr)O_3$ thin films. In the $(Ba,Pb)(Ti,Zr)O_3$ thin films system, the solid solution $x BaZrO_3$-$(1-x)PbTiO_3$ with $x = 0.45$ has been successfully fabricated by rf

* Corresponding author. Tel.: +886-62585663; fax: +886-62502734.

0955-2219/03/$ - see front matter © 2003 Elsevier Ltd. All rights reserved.
doi:10.1016/S0955-2219(03)00039-6

magnetron sputtering and the crystallization behavior of this amorphous thin film for rapid thermal annealing has been studied by Torii.[12] However, the studies of the deposition parameters on the dielectric properties of the rf magnetron sputtered $Ba(Z_xT_{1-x})O_3$ (BZ_xT_{1-x}) thin films have not been elucidated.

In the present investigation, the influence of the deposition parameters on the dielectric properties of the BZ_xT_{1-x} thin films deposited by rf magnetron sputtering have been studied using X-ray diffraction (XRD) and capacitance-voltage measurements.

2. Experimental procedure

2.1. Sample preparation

The stoichiometric $Ba(Zr_xTi_{1-x})O_3$ ceramic targets with various x values were prepared as follows. The chemical composition of ceramic targets was listed in Table 1. Commercial $BaZrO_3$ (purity 99.0%, supplied by Johnson Matthey Inc., West Chester, PA, USA) and $BaTiO_3$ (purity 99.0%, supplied by Noah Tech. Co., San Antonio Texas, USA) were weighed and ball-milled with acetone and alumina balls for 10 h, dried by an infrared lamp, and subsequently ground and sieved. The powders have been put through an 80-mesh sieve and were then mixed with 1.0 wt.% polyvinyl acetate (PVA) binder and pressed at 180 MPa to form a disk of 5.0 cm in diameter. Sintering of the samples was conducted at a heating rate of 4.5 °C min^{-1} after the binder was burned out at 600 °C for 30 min. The samples were then heated at 1.5 °C min^{-1} to 1100 °C and held for 2 h. Finally, the sintered samples were then cooled to room temperature at a rate of 3 °C min^{-1}.

The *n*-Si(100) wafer substrate was cleaned by a standard process. The substrate has a dimension of $10.0\times10.0\times0.50$ mm^3. A high quality silicon oxide layer was grown by thermal oxidation to obtain a 200.0 nm thin film. The capacitor structure comprised platinum (Pt) top and bottom electrodes with a 5.0 nm Ti film deposited by rf magnetron sputtering from a Ti target for increases adhesion. The 500.0 nm thin Pt bottom electrode was sputter-deposited at 400 °C. Both metals were sputtered in an Ar atmosphere at working pressure (W_p) of 1.0×10^{-2} Torr with an applied power of 150 W.

Table 1
Chemical composition of the stoichiometric ceramic targets for the preparation $Ba(Ti_{1-x}Zr_x)O_3$ thin films

Starting material	Sample notation and composition (mol.%)		
	$BZ_{0.1}T_{0.9}$	$BZ_{0.2}T_{0.8}$	$BZ_{0.3}T_{0.7}$
$BaZrO_3$	10	20	30
$BaTiO_3$	90	80	70

The BZ_xT_{1-x} thin films with various x values were deposited on the $Pt/Ti/SiO_2$ /Si substrates by rf magnetron sputtering. The sputtering apparatus is schematically shown in Fig. 1. The overall sputtering parameters for the preparation of the BZ_xT_{1-x} thin films are listed in Table 2. The Pt top electrodes with a thickness of 50.0 nm and diameters of 150.0, 250.0 and 350.0 nm were patterned by a shadow mask process. The schematic of the BZ_xT_{1-x} thin films capacitor is shown in Fig. 2.

2.2. Films characterization and dielectric properties measurement

The thickness of the BZ_xT_{1-x} thin films with various x values was determined using an Automatic Ellipsometer (Rudolph Research Co.) with a He-Ne laser (wavelength (λ) = 6328 Å) as a detecting probe as well as with a Tencor Alpha-Step 200 profilometer. The BZ_xT_{1-x} thin films had the composition range of x from 0.1 to 0.3 and thickness remained around 500.0 nm.

The phase identification of the BZ_xT_{1-x} thin films samples were examined using an X-ray diffractionmeter (XRD) with Cu K_α radiation and a Ni filter, operated at 30 kV, 20 mA and a scanning rate of 0.25 degree min^{-1} (Model Rad IIA, Rigaku Co., Tokyo, Japan).

The morphology of the cross section of the $BZ_{0.3}T_{0.7}$ thin films was examined by a scanning electron microscope (SEM) (Model S-4200, Hitachi Ltd., Tokyo, Japan). The composition was analyzed with energy dispersive spectrometry (EDS) (Model Noran Vantage, USA) employing an internal standard method.

Dielectric constant-temperature curves from 20 to 160 °C were measured at ac voltage = 1 V and frequency = 1 kHz, using an HP 4192 A LF impedance analyzer with a mini-subzero MC-81 thermostat. The dielectric constant (ε_r) was obtained from Eq. (1):

$$\varepsilon_r = Cd(A\varepsilon_o)^{-1} \quad (1)$$

where C is the capacitance (farad), d is the film thickness (m), A is the area of a Pt top electrode (m^2) and ε_o is the permittivity of free space (8.854×10^{-12} farad m^{-1}).

Table 2
Rf magnetron sputtering parameters for the $Ba(Ti_{1-x}Zr_x)O_3$ thin films

Target diameter (cm)	5.0
Target-substrate distance (cm)	3.6
Background pressure (10^{-5} Torr)	2
Working pressure (10^{-5} Torr)	5–15
Sputtering gas	Ar or (O_2 + Ar) gas
Rf power (W)	100–160
Substrate temperature (°C)	300–500
Deposition time (min)	60
Film thickness (nm)	500

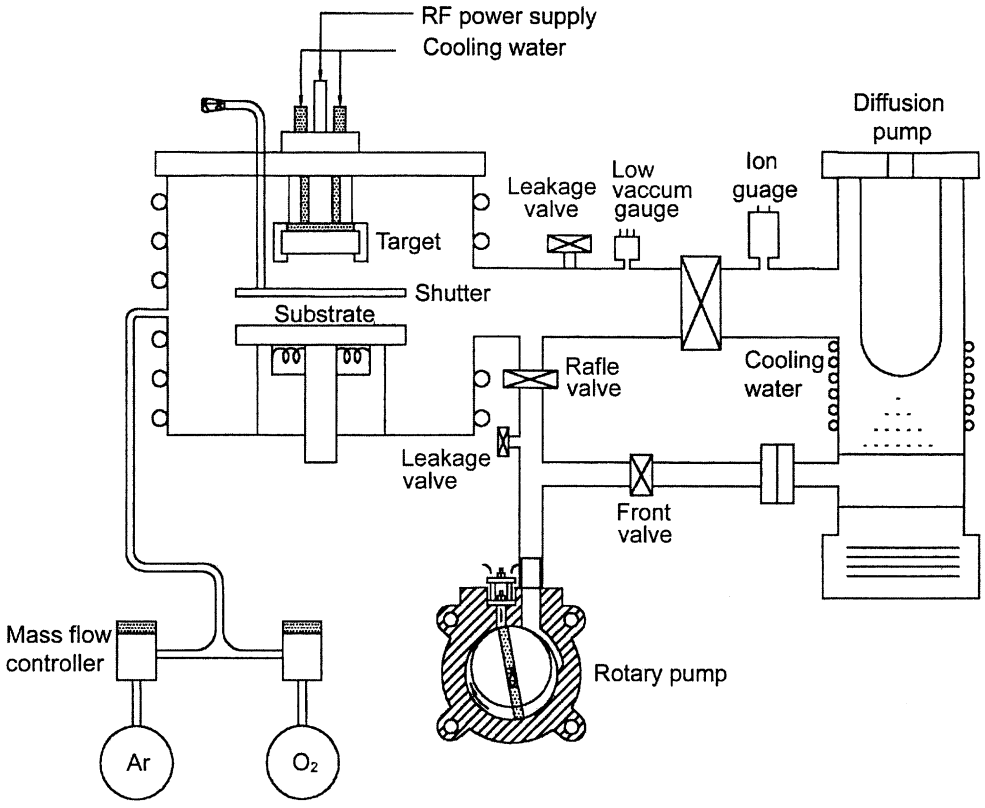

Fig. 1. Schematic diagram of the rf magnetron sputtering apparatus for the preparation the BZ_xT_{1-x} thin films.

3. Results and discussion

3.1. Crystal structure and chemical composition of the BZ_xT_{1-x} thin films

At the $R_p = 100$ W, $W_p = 1.0\times10^{-2}$ Torr and $O_2\cdot(O_2 + Ar)^{-1}$ ratio $(O_r) = 1\cdot(1+9)^{-1}$, the XRD patterns of the $BZ_{0.3}T_{0.7}$ ($x = 0.3$) sputtered at various temperatures are shown in Fig. 3. It indicates that the $BZ_{0.3}T_{0.7}$ thin films are amorphous in addition to the strong Si (200) and Pt (111) reflections when sputtered at 300 °C. This phenomenon is a consequence of the low kinetic energy of the sputter-ejected species for atomic arrangement and crystallization when sputtered at low rf power and substrate temperature.

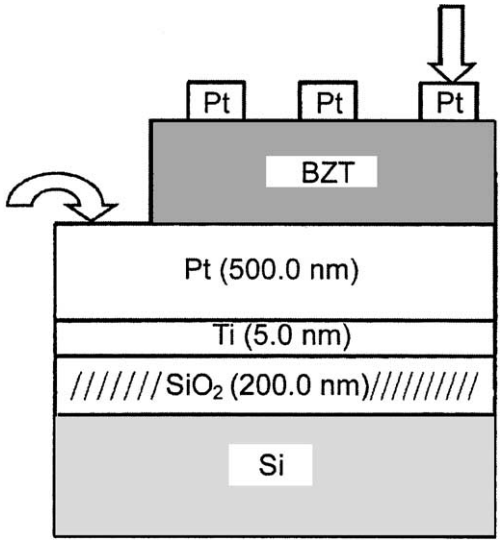

Fig. 2. Schematic cross section of the BZ_xT_{1-x} thin film capacitor.

The crystalline phase of BZT appears in the $BZ_{0.3}T_{0.7}$ thin film when the substrate temperature increases from 300 to 400 and 500 °C, respectively [see Fig. 3(b) and (c)]. The intensity of the BZT (100) and (200) reflections increases with increasing substrate temperature. This result is caused by the kinetic energy of the sputtered-ejected species leading to the atomic arrangement and film crystallization on the substrate. From Fig. 3(b) and (c), it is observed that only the BZT (h00) reflections take place and this result indicates that the thin film consists of a single BZT phase and is grown on the substrate. In addition, the strong Pt (111) reflection is found. This phenomenon demonstrates that the BZT (100) plane is parallel to the Pt (111) plane.[8]

When the $R_p = 130$ W, $S_T = 300$ °C and $O_r = 1\cdot(1+9)^{-1}$, the XRD patterns of the $BZ_{0.3}T_{0.7}$ thin films shown in Fig. 4 are the same as in Fig. 3. This result indicates that the $BZ_{0.3}T_{0.7}$ thin film has a high degree of (100) preferred orientation, irrespective of the sputtering working pressure. On the other hand, Fig. 4 also shows that the crystallinity of the $BZ_{0.3}T_{0.7}$ thin

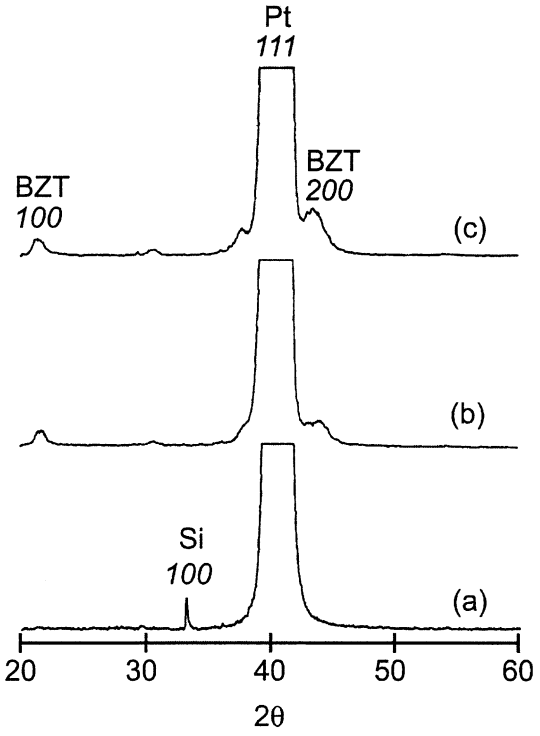

Fig. 3. XRD patterns of the $BZ_{0.3}T_{0.7}$ thin film sputtered at $R_p = 100$ W, $W_p = 1.0\times10^{-2}$ Torr, $O_r = 1\cdot(1+9)^{-1}$and various substrate temperatures: (a) 300 °C, (b) 400 °C and (c) 500 °C.

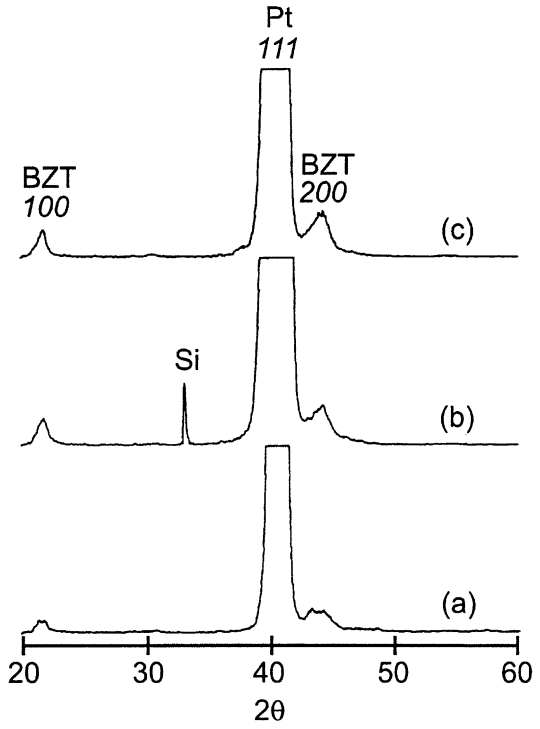

Fig. 4. XRD patterns of the $BZ_{0.3}T_{0.7}$ thin film deposited at $R_p = 160$ W, $S_T = 300$ °C, $O_r = 1\cdot(1+9)^{-1}$ and different work pressure: (a) 15×10^{-3} Torr, (b) 10×10^{-3} Torr and (c) 5.0×10^{-3} Torr.

film decreases with increasing working pressure. This phenomenon is caused because during sputtering, the target atoms are subject to collisions with ambient gas atoms and other ejected atoms resulting in a partial loss of energy and direction on their way to the substrate. The motion of both sputtered atoms and ions is thus impeded by the sputtering gas pressure.[17] At a given rf power the thermalization region shifts towards the target by increasing working pressure. This results in the oxidation of the target[18,19] and possible resputtering of the films.[20]

Fig. 5 shows the effect of O_r and Zr content on the $Zr\cdot(Zr+Ti)^{-1}$ ratio of the BZ_xT_{1-x} thin films deposited on the $Pt/Ti/SiO_2/Si$ substrate at $R_p = 130$W, $W_p = 5.0\times10^{-3}$ Torr and $S_T = 500$ °C. It indicates that the $Zr\cdot(Zr+Ti)^{-1}$ ratio of the films is slightly greater than the target irrespective of the $O_2\cdot(O_2+Ar)^{-1}$ ratio. This result is caused by the both sputtering and sticking coefficient of Zr are greater than Ti. Since the materials sputtered from the target may collide with gas atoms (O_2, Ar) on their way to the substrate, the heavy atoms rather that the light atoms reach the substrate.[11] At pressures as high as 10–30 Pa (0.075–0.226 Torr), the mean free path of the sputtered atoms and ions is in the order of millimeter, thus, the impingement of high-energy particles is reduced and the compositional change is suppressed.[11]

3.2. Dielectric properties of the BZ_xT_{1-x} thin films

When the $W_p = 5.0\times10^{-3}$ Torr, $O_r = 1\cdot(1+9)^{-1}$ and $S_T = 400$ °C, the effect of the measurement temperature

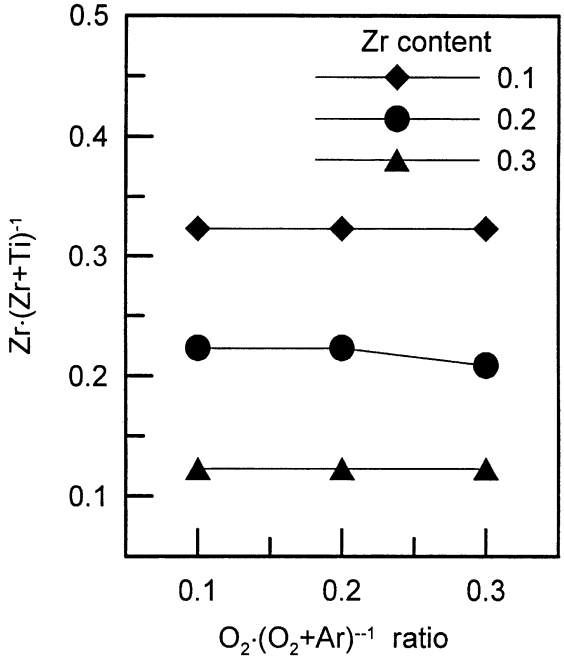

Fig. 5. Effect of the $O_2\cdot(O_2+Ar)^{-1}$ ratio and Zr content on the $Zr\cdot(Zr+Ti)^{-1}$ ratio of the BZ_xT_{1-x} thin films deposited at $R_p = 130$ W, $W_p = 5.0\times10^{-3}$ Torr and $S_T = 500$ °C.

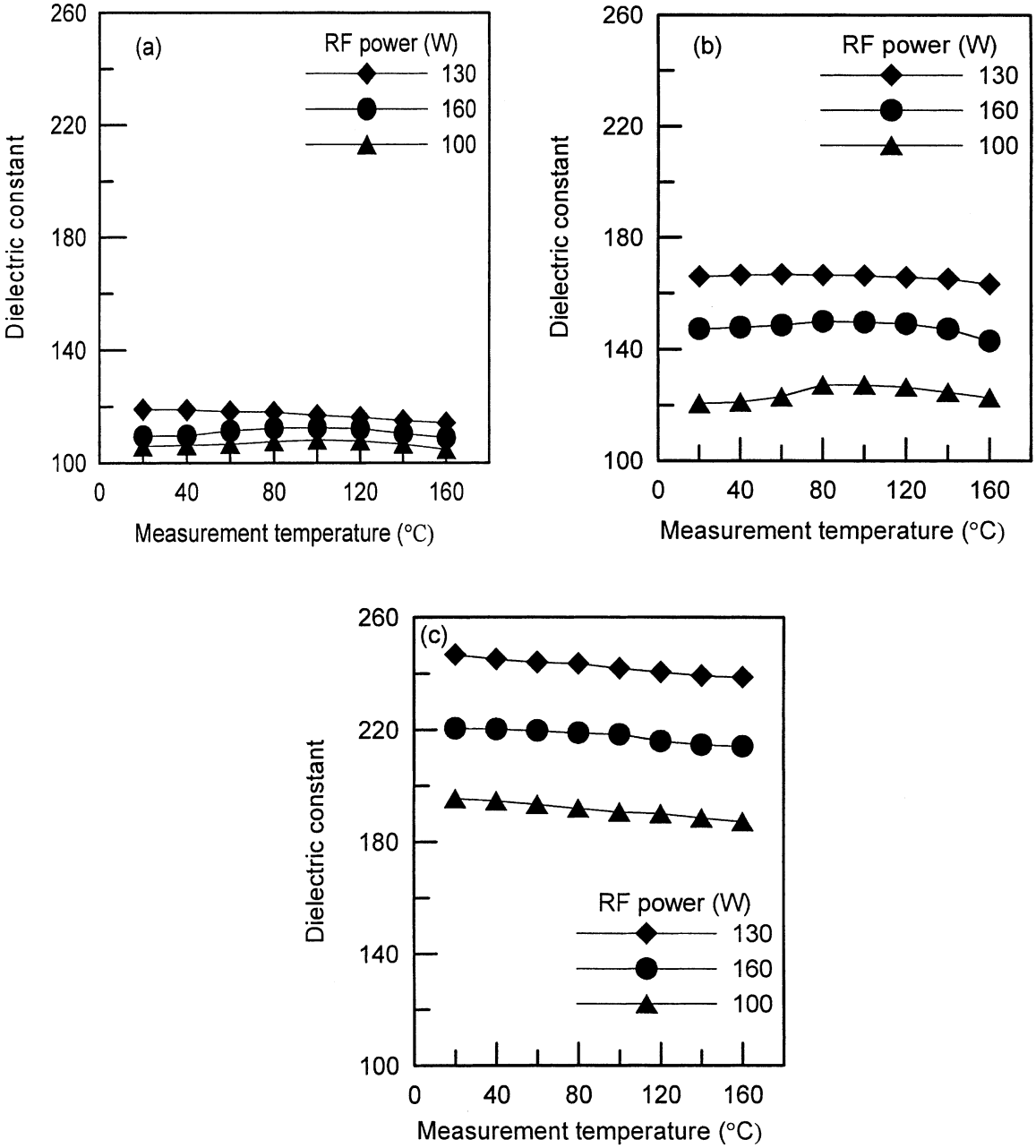

Fig. 6. Effect of the measurement temperature, rf power and Zr content on the dielectric constant of the BZ_xT_{1-x} thin films deposited at $W_p = 5.0\times10^{-3}$ Torr, $O_r = 1\cdot(1+9)^{-1}$ and $S_T = 400$ °C: (a) $BZ_{0.1}T_{0.9}$ thin films ($x = 0.1$), (b) $BZ_{0.2}T_{0.8}$ thin films ($x = 0.2$) and (c) $BZ_{0.3}T_{0.7}$ thin films ($x = 0.3$).

and rf power on the dielectric constant of the BZ_xT_{1-x} thin films with various x values are shown in Fig. 6. It indicates that the dielectric constant decreases with increasing measurement temperature, irrespective of the rf power and Zr content of the BZ_xT_{1-x} thin films. It is also found that when the rf power is 130 W, the dielectric constant has a maximum value, irrespective of the Zr content of the BZ_xT_{1-x} thin films.

Since the variation of the dielectric constant of the BZ_xT_{1-x} thin films with various x values has the same trend, the present study about the influence of the deposition parameters on the dielectric properties of the BZ_xT_{1-x} thin films has been focused on the $BZ_{0.3}T_{0.7}$ thin film.

The effect of the Zr content on the dielectric constant and loss tangent (tan δ) of the $BZ_{0.3}T_{0.7}$ thin film deposited on the $Pt/Ti/SiO_2/Si$ substrate at $R_p = 130$ W, $W_p = 5.0\times10^{-3}$ Torr, $O_r = 1\cdot(1+9)^{-1}$ and $S_T = 500$ °C are shown in Fig. 7. It indicates that tanδ insignificantly increases with increasing Zr content. But the dielectric constant of the BZ_xT_{1-x} thin film shows a sudden increase from 124.1 to 280.2 with the Zr content

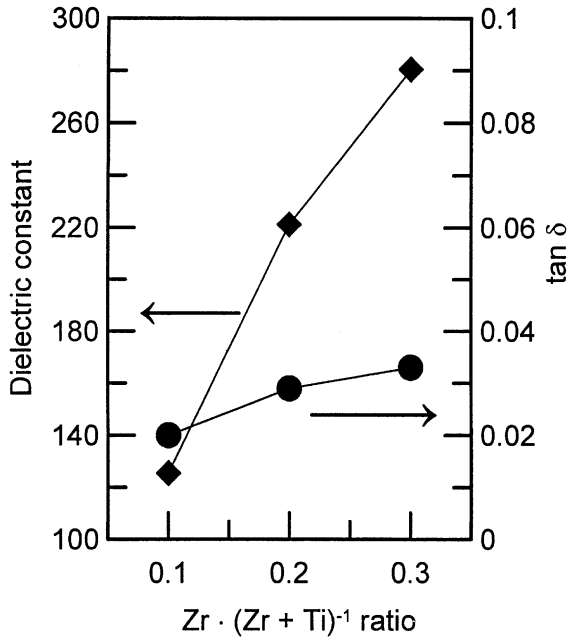

Fig. 7. Effect of the Zr content on the dielectric constant and loss tangent of the $BZ_{0.3}T_{0.7}$ thin film deposited at $R_p = 130$ W, $W_p = 5.0\times10^{-3}$ Torr, $O_r = 1\cdot(1+9)^{-1}$ and $S_T = 500$ °C.

increasing from $x = 0.1$ to 0.3. As the $BZ_{0.25}T_{0.75}$ ceramic is known to have the Curie point of room temperature,[21] the maximum dielectric constant is expected to be at room temperature. This results suggests the decrease of the Curie temperature of the sputtered BZ_xT_{1-x} thin films is by 100 °C for $x = 0.3$.

Fig. 8 shows the effect of the rf power on the dielectric constant and tan δ when the $BZ_{0.3}T_{0.7}$ thin film sputtered at $W_p = 5\times10^{-3}$ Torr, $O_r = 1\cdot(1+9)^{-1}$ and $S_T = 500$ °C. It can be found that the effect of the rf power on tan δ is very slight. But the dielectric constant of the $BZ_{0.3}T_{0.7}$ thin films increases from 244.0 to 284.1 with the rf power increased from 100 to 130 W. On the other hand, the dielectric constant decreases from 284.1 to 270.0 when the rf power increases from 130 to 160 W.[22] This result can be caused by resputtering.[20] The macro effect of resputtering includes slowing of film deposition rate and, in some cases, complete suppression of film growth as well as etching of substrate materials. Rf power has an important influence on resputtering when it is so high that it causes both deposition and etching at the same time.[20] When rf power increases from 130 to 160 W, the increased resputtering process and leads to decreased the dielectric constant.

Fig. 9 shows the effect of the deposition temperature on the dielectric constant and tan δ of the $BZ_{0.3}T_{0.7}$ capacitors. The $BZ_{0.3}T_{0.7}$ thin film is sputter deposited at $R_p = 130$ W, $W_p = 5.0\times10^{-3}$ Torr and $O_r = 1\cdot(1+9)^{-1}$. It indicates that the $BZ_{0.3}T_{0.7}$ thin film has a small dielectric loss tangent and the dielectric constant increases from 164.7 to 283.7 with the deposition temperature increased from 300 to 500 °C. According to Fig. 3, when the substrate temperature increases from 300 to 500 °C at $R_p = 100$ W, the $BZ_{0.3}T_{0.7}$ thin film transforms from amorphous to a single $BaZr_xTi_{1-x}O_3$ phase. When the deposition temperature increases from 300 to 500 °C at R_p 130 W, the $BZ_{0.3}T_{0.7}$ thin film has the (100) preferred orientation and the crystallinity suddenly increases with increasing substrate tempera-

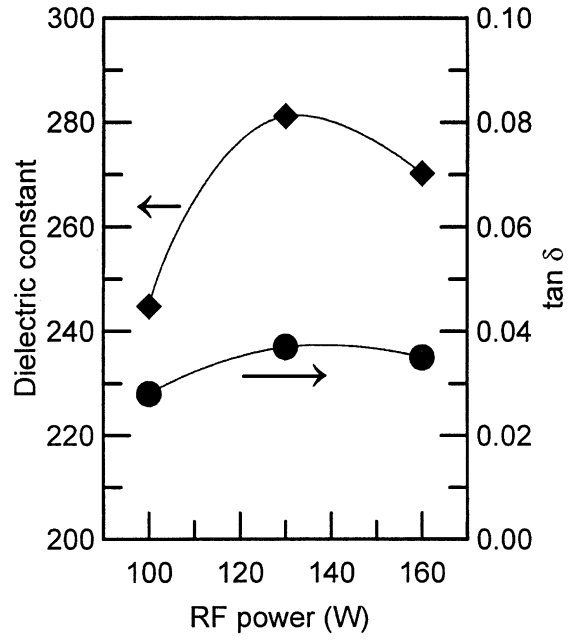

Fig. 8. Effect of the rf power on the dielectric constant and tan δ of the $BZ_{0.3}T_{0.7}$ thin film deposited at $W_p = 5.0\times10^{-3}$ Torr, $O_r = 1\cdot(1+9)^{-1}$ and $S_T = 500$ °C.

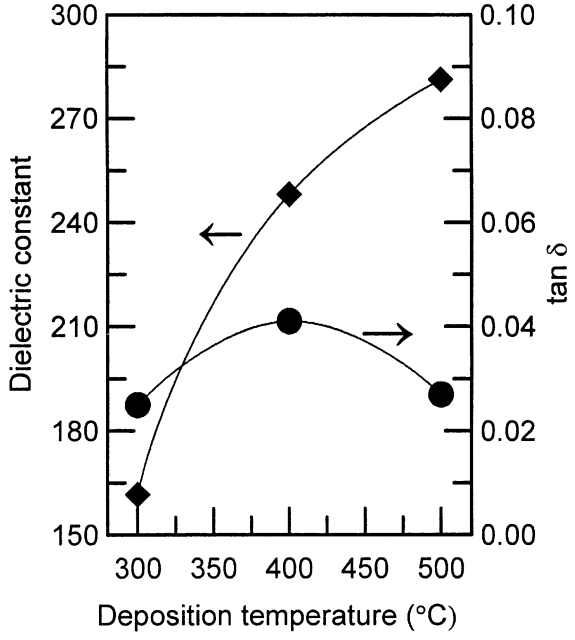

Fig. 9. Effects of the deposition temperature on the dielectric constant and tan δ of the $BZ_{0.3}T_{0.7}$ thin film deposited at $R_p = 130$ W, $W_p = 5\times10^{-3}$ Torr and $O_r = 1\cdot(1+9)^{-1}$ and $S_T = 500$ °C.

ture.[22] According to Figs. 3, 8 and 9, the dielectric constant increases with increasing substrate temperature that leads to increase crystallinity of the thin films.

When the $BZ_{0.3}T_{0.7}$ thin film is sputtered at $R_p = 130$W, $O_r = 1\cdot(1+9)^{-1}$ and $S_T = 500$ °C, the relationships among the working pressure, dielectric constant and tan δ of the $BZ_{0.3}T_{0.7}$ capacitors are shown in Fig. 10. It indicates that the $BZ_{0.3}T_{0.7}$ thin film also has a small tan δ with the working pressure ranging from 5.0×10^{-3} to 15×10^{-3} Torr and the variation is also similar to the effect of the deposition temperature. The dielectric constant also decreases from 281.5 to 232.6 while working pressure is increasing from 5.0×10^{-3} to 15×10^{-3} Torr. According to Fig. 4, the crystallization of the $BZ_{0.3}T_{0.7}$ thin film decreases with increasing working pressure. Besides, the deposition rate of the BZ_xT_{1-x} thin films also decreases with increasing working pressure.[22] These results reveal that the crystallinity of the BZ_xT_{1-x} thin films are degenerated by resputtering and leads to the dielectric constant decrease with increasing working pressure.

When the $R_p = 130$ W, $W_p = 5\times10^{-3}$ Torr and $S_T = 500$ °C, the effects of the $O_2\cdot(O_2+Ar)^{-1}$ ratio on the dielectric constant and tan δ are shown in Fig. 11. Although the $BZ_{0.3}T_{0.7}$ thin film has a small tan δ that decreases with increasing $O_2\cdot(O_2+Ar)^{-1}$ ratio. It is also found that the dielectric constant is very low, only 164.1, when the sputtering gas does not contain oxygen. When the sputtering gas contains 10% O_2, the dielectric constant suddenly increases from 164.1 to 281.5. When the sputtering gas contain 20% O_2, the dielectric constant has an insignificant variation. This result is caused by oxygen addition that enhances the crystallization of the $BZ_{0.3}T_{0.7}$ thin film[22] and leads to the increase of the dielectric constant.

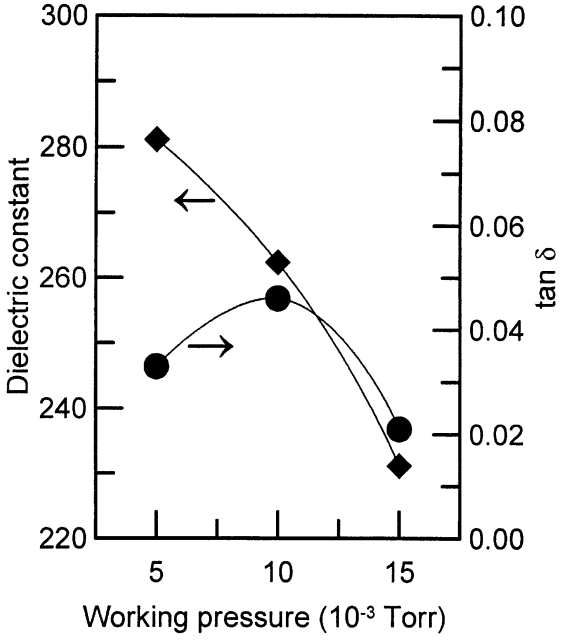

Fig. 10. Relationships among the working pressure, dielectric constant and tan δ of the $BZ_{0.3}T_{0.7}$ thin film deposited at $R_p = 130$ W, $O_r = 1\cdot(1+9)^{-1}$ and $S_T = 500$ °C.

3.3. SEM micrographs of the BZT films

When the $R_p = 130$ W, $W_p = 5\times10^{-3}$ Torr, $O_r = 1\cdot(1+9)^{-1}$ and $S_T = 500$ °C, the SEM micrograph of the $BZ_{0.3}T_{0.7}$ thin film is shown in Fig. 12. The film exhibits obviously a columnar grain structure and its surface appears smooth and dense without any microcracks.

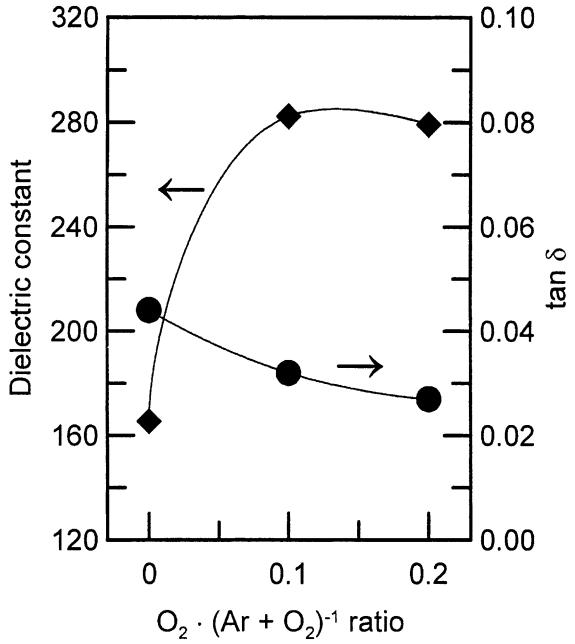

Fig. 11. Effect of the $O_2\cdot(O_2+Ar)^{-1}$ ratio on the dielectric constant and tan δ of the $BZ_{0.3}T_{0.7}$ thin film deposited at $R_p = 130$ W, $W_p = 5\times10^{-3}$ Torr and $S_T = 500$ °C.

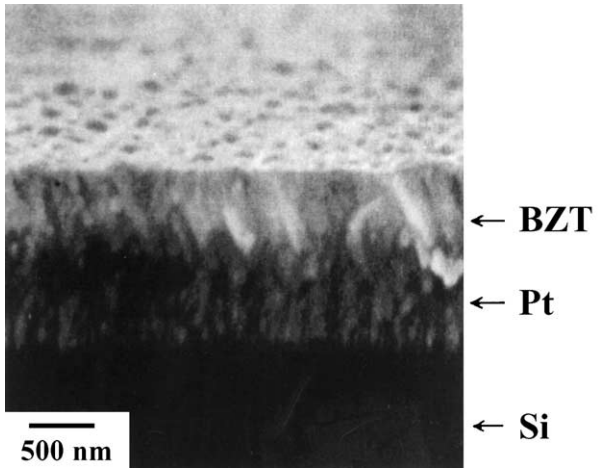

Fig. 12. SEM micrograph of the $BZ_{0.3}T_{0.7}$ thin film deposited at $R_p = 130$ W, $W_p = 5\times10^{-3}$, $O_r = 1\cdot(1+9)^{-1}$ and $S_T = 500$ °C.

4. Conclusions

The $Ba(Zr_xTi_{1-x})O_3$ (BZ_xT_{1-x}) thin films with $0.1 \leqslant x \leqslant 0.3$ have been deposited on the $Pt/Ti/SiO_2/Si$ substrates by rf magnetron sputtering. The results in this study are summarized as follows:

1. The $BZ_{0.3}T_{0.7}$ thin film is amorphous when sputtered at $R_p = 100$ W, $W_p = 1.0\times10^{-2}$ Torr, $O_r = 1\cdot(1+9)^{-1}$ and $S_T = 300$ °C. The crystalline $BZ_{0.3}T_{0.7}$ thin film appears when the substrate temperature increases from 300 to 400 and 500 °C, respectively. The $BZ_{0.3}T_{0.7}$ thin film has a high degree of (100) preferred orientation, irrespective of the working pressure, and the crystallinity of the $BZ_{0.3}T_{0.7}$ thin film decreases with increasing working pressure.
2. The $Zr\cdot(Zr+Ti)^{-1}$ ratio of the thin film is slightly greater than the target irrespective of the $O_2\cdot(O_2+Ar)^{-1}$ ratio.
3. The dielectric constant decreases with increasing measurement temperature, irrespective of the rf power and the Zr content of the BZ_xT_{1-x} thin films with various x values. The $BZ_{0.3}T_{0.7}$ thin film has a same dielectric constant and loss tangent irrespective of the sputtering parameters.
4. The dielectric constant increases with increasing $Zr\cdot(Zr+Ti)^{-1}$ ratio and deposition temperature, but decreases with increasing working pressure. The dielectric constant also increases from 244.0 to 284.1 with the rf power increased from 100 to 130 W and then it decreases from 284.1 to 270.0 when the rf power increases from 130 to 160 W. The dielectric constant suddenly increases from 164.1 to 281.5 when the sputtering gas contains O_2 from 0 to 10%, but only insignificant variation is observed when the sputtering gas contains 20% O_2.
5. The $BZ_{0.3}T_{0.7}$ thin film exhibits obviously the columnar grain structure, and it surface appears smooth and dense without any microcrack.

Acknowledgements

This work was supported by National Science Council, Taiwan, the Republic of China under Contract No. NSC89-2216-E-151-004 which is gratefully acknowledged. Help in experimental works and suggestions from Professor M.P. Hung, Professor M.H. Hon, Mr. S.Y. Yau and Mr. J.M. Chen are appreciated.

References

1. Li, P. and Lu, T. M., Conduction mechanisms in $BaTiO_3$ thin films. *Phys. Rev.*, 1991, **43**, 14261–14264.
2. Ray, D. and Krupanidhi, S. B., Pulsed excimer laser ablated barium titanate thin films. *Appl. Phys. Lett.*, 1992, **61**, 2057–2059.
3. Gerblinger, J. and Meixnor, H., Electrical conductivity of sputtered films of strontium titanate. *J. Appl. Phys.*, 1990, **67**, 7453–7459.
4. Yamaguchi, H., Lesaicherre, P. Y., Sakuma, T., Miyasaka, Y., Ishitani, A. and Yoshida, M., Structural and electrical characterization of $SrTiO_3$ thin films prepared by metal organic chemical vapor deposition. *Jpn. J. Appl. Phys. 1*, 1993, **32**, 4069–4073.
5. Abe, Y., Kawamura, M. and Sasaki, K., Dielectric properties of $SrTiO_3$ capacitor using TiN bottom electrode and effects of $SrTiO_3$ film thickness. *Jpn. J. Appl. Phys. 1*, 1997, **36**, 5175–5178.
6. Kamatsu, S., Abe, K. and Fukushima, N., Effect of ambient gas on dielectric constant of sputtered $SrTiO_3$ epitaxial thin films. *Jpn. J. Appl. Phys. 1*, 1998, **37**, 5651–5654.
7. Horikawa, T., Mikami, N., Makita, T., Tanimura, J., Kataoka, M., Sato, K. and Nunoshita, M., Dielectric properties of $(Ba,Sr)TiO_3$ thin films deposited by rf sputtering. *Jpn. J. Appl. Phys. 1*, 1993, **32**, 4126–4130.
8. Abe, K. and Komatsu, S., Ferroelectric properties in epitaxially grown of $Ba_xSr_{1-x}TiO_3$ thin films. *J. Appl. Phys.*, 1995, **77**, 6461–6465.
9. Tsurumi, T., Miyasou, T., Ishibashi, Y. and Ohashi, N., Prepartion and dielectric property of $BaTiO_3$– $SrTiO_3$ artificially modulated structures. *Jpn. J. Appl. Phys. 1*, 1998, **37**, 5104–5107.
10. Hu, H. and Krupamidhi, S. B., Property modification of ferroelectric $Pb(Zr,Ti)O_3$ thin films by low-energy oxygen ion bombardment during film growth. *Appl. Phys. Lett.*, 1992, **61**, 1246–1248.
11. Torii, K., Kaga, T. and Takeda, E., Dielectric properties of rf magnetron-sputtered $(Ba,Pb)(Zr,Ti)O_3$ thin films. *Jpn J. Appl. Phys. 1*, 1992, **31**, 2989–2991.
12. Torii, K., Dielectric properties of rf magnetron-sputtered $(Ba,Pb)(Zr,Ti)O_3$ thin films. *Ferroelectrics*, 1994, **152**, 157–162.
13. Cha, S. Y., Lee, S. H. and Lee, H. C., Ti thickness effect in Pt/Ti bottom electrode on properties of $(Ba,Sr)TiO_3$ thin film. *Integrated Ferroelectrics*, 1997, **16**, 183–190.
14. Wang, Y. P. and Tseng, T. Y., Electronic defect and trap-related current of $(Ba_{0.4}Sr_{0.6})TiO_3$ thin films. *J. Appl. Phys*, 1997, **81**, 6762–6766.
15. Baumert, B. A., Chang, L. H., Matsuda, A. T., Tsai, T. L., Tracy, C. J., Gregory, R. B., Fejes, P. L., Cave, N. G., Chen, W., Taylor, C. J., Otsuki, T., Fujii, E., Hayashi, E. S. and Suu, K., Characterization of sputtered barium strontium titanate and strontium titanate-thin films. *J. Appl. Phys.*, 1997, **82**, 2558–2566.
16. Krupanidhi, S. B., Hu, H. and Kumar, V., Multi-ion-beam reactive sputter deposition of ferroelectric $Pb(Zr,Ti)O_3$ thin films. *J. Appl. Phys.*, 1992, **71**, 376–388.
17. Tahar, R. B. H., Ban, T., Ohya, Y. and Takahashi, Y., The doped indium oxide thin films: electrical properties. *J. Appl. Phys.*, 1998, **83**, 2631–2645.
18. Leja, E., Kolodiez, A., Pisarkiewiez, T. and Stapinski, T., The dynamics of reactive ion sputtering of Sn–Sb and In–Sn alloys in an $Ar–O_2$ atmosphere. *Thin Solid Films*, 1981, **76**, 283–287.
19. Buchanan, M., Webb, J. B. and Williams, D. F., The influence of target oxidation and growth related effects on the electrical properties of reactively sputtered films on tin-doped indium oxide. *Thin Solid Films*, 1981, **81**, 373–382.
20. Kester, D. J. and Messier, R., Macro-effects of resputtering due to negative ion bombardment of growing thin films. *J. Mater. Res.*, 1993, **8**, 1928–1937.
21. Neirman, S. M., The Curie point temperature of $Ba(Ti_{1-x}Zr_x)O_3$ solid solution. *J. Mater. Sci.*, 1998, **23**, 3973–3980.
22. Wang, M. C., Chen, C. Y., His, C. S. and Wu, N. C., Deposition characteristics of $Ba(Ti_{1-x}Zr_x)O_3$ thin films prepared by rf magnetron sputtering. *J. Crystal Growth*, 2002, **246**, 99–107.